



**NAVAL
POSTGRADUATE
SCHOOL**

MONTEREY, CALIFORNIA

THESIS

**HEAT CONDUCTION ANALYSIS OF RANDOMLY
DISPERSED SINGLE-WALLED CARBON NANOTUBES**

by

Eric D. Felder

June 2007

Thesis Advisor:

Young W. Kwon

Approved for public release; distribution is unlimited

THIS PAGE INTENTIONALLY LEFT BLANK

REPORT DOCUMENTATION PAGE			<i>Form Approved OMB No. 0704-0188</i>
Public reporting burden for this collection of information is estimated to average 1 hour per response, including the time for reviewing instruction, searching existing data sources, gathering and maintaining the data needed, and completing and reviewing the collection of information. Send comments regarding this burden estimate or any other aspect of this collection of information, including suggestions for reducing this burden, to Washington headquarters Services, Directorate for Information Operations and Reports, 1215 Jefferson Davis Highway, Suite 1204, Arlington, VA 22202-4302, and to the Office of Management and Budget, Paperwork Reduction Project (0704-0188) Washington DC 20503.			
1. AGENCY USE ONLY (Leave blank)	2. REPORT DATE June 2007	3. REPORT TYPE AND DATES COVERED Master's Thesis	
4. TITLE AND SUBTITLE: Heat Conduction Analysis of Randomly Dispersed Single-Walled Carbon Nanotubes		5. FUNDING NUMBERS	
6. AUTHOR(S) Eric D. Felder		8. PERFORMING ORGANIZATION REPORT NUMBER	
7. PERFORMING ORGANIZATION NAME(S) AND ADDRESS(ES) Naval Postgraduate School Monterey, CA 93943-5000		10. SPONSORING/MONITORING AGENCY REPORT NUMBER	
9. SPONSORING /MONITORING AGENCY NAME(S) AND ADDRESS(ES) N/A		11. SUPPLEMENTARY NOTES The views expressed in this thesis are those of the author and do not reflect the official policy or position of the Department of Defense or the U.S. Government.	
12a. DISTRIBUTION / AVAILABILITY STATEMENT Approved for public release; distribution is unlimited		12b. DISTRIBUTION CODE	
13. ABSTRACT (maximum 200 words) This thesis studies the effective thermal conductivity of randomly oriented, percolated carbon nanotubes. To that end, a multiscale analysis approach was adopted. At the nanoscale, molecular dynamics simulation was performed to determine the thermal conductivity coefficient of a single carbon nanotube. Then, thermal conductivity of two carbon nanotubes positioned at different angles were studied after determining the equilibrium positions of the two nanotubes at various relative positions. Finally, using the data obtained in the previous analyses, the effective thermal conductivity of randomly oriented carbon nanotubes was calculated using the finite element model where each nanotube was modeled as a continuous rod.			
14. SUBJECT TERMS Molecular Dynamics, Carbon Nanotubes, SWNT, CNT, Tersoff-Brenner Potential, Lennard Jones Potential			15. NUMBER OF PAGES 53
			16. PRICE CODE
17. SECURITY CLASSIFICATION OF REPORT Unclassified	18. SECURITY CLASSIFICATION OF THIS PAGE Unclassified	19. SECURITY CLASSIFICATION OF ABSTRACT Unclassified	20. LIMITATION OF ABSTRACT UL

NSN 7540-01-280-5500

Standard Form 298 (Rev. 2-89)
Prescribed by ANSI Std. Z39-18

THIS PAGE INTENTIONALLY LEFT BLANK

Approved for public release, distribution is unlimited

**HEAT CONDUCTION ANALYSIS OF RANDOMLY DISPERSED SINGLE-
WALLED CARBON NANOTUBES**

Eric D. Felder
Lieutenant, United States Navy
B.S., Florida A & M University, 1999

Submitted in partial fulfillment of the
requirements for the degree of

MASTER OF SCIENCE IN MECHANICAL ENGINEERING

from the

**NAVAL POSTGRADUATE SCHOOL
June 2007**

Author: Eric D. Felder

Approved by: Young W. Kwon
Thesis Advisor

Anthony J. Healey
Chairman, Department of Mechanical and Astronautical
Engineering

THIS PAGE INTENTIONALLY LEFT BLANK

ABSTRACT

This thesis studies the effective thermal conductivity of randomly oriented, percolated carbon nanotubes. To that end, a multiscale analysis approach was adopted. At the nanoscale, molecular dynamics simulation was performed to determine the thermal conductivity coefficient of a single carbon nanotube. Then, thermal conductivity of two carbon nanotubes positioned at different angles were studied after determining the equilibrium positions of the two nanotubes at various relative positions. Finally, using the data obtained in the previous analyses, the effective thermal conductivity of randomly oriented carbon nanotubes was calculated using the finite element model where each nanotube was modeled as a continuous rod.

THIS PAGE INTENTIONALLY LEFT BLANK

TABLE OF CONTENTS

I.	INTRODUCTION.....	1
A.	BACKGROUND	1
B.	OBJECTIVES	4
II.	MODELING, RELATED THEORY, AND METHODOLOGY	7
A.	LABORATORY SYNTHESIS OF CARBON NANOTUBES.....	7
B.	MD THEORY AND TERSOFF-BRENNER (T-B) POTENTIAL.....	8
1.	Validity of the Classical MD Simulation Method	8
2.	Newton-Hamiltonian Dynamics for the Classical MD Simulation.....	9
3.	Tersoff-Brenner (T-B) Type Potential	10
4.	Gear's Predictor-Corrector Method for Solving the EOM	13
a.	Prediction	13
b.	Evaluation	14
c.	Correction.....	14
5.	Simulation Time Step	14
C.	EQUILIBRIUM MOLECULAR DYNAMICS USING AUTO-CORRELATION FORMULA (GREEN-KUBO FORMULA)	15
D.	LENNARD-JONES POTENTIAL	16
III.	SIMULATION	17
A.	MODELING OF SWNT AND BASIC STRUCTURES.....	17
1.	Basic Structures of Carbon Nanotubes.....	17
2.	SWNT Model.....	18
B.	SIMULATION PROCEDURES.....	20
1.	Thermal Conductivity Coefficient of a Single Carbon Nanotube.....	20
2.	Thermal Conductivity of Two Carbon Nanotubes	21
3.	Effective Thermal Conductivity	22
IV.	RESULTS AND DISCUSSION	25
A.	THERMAL TRANSFER COEFFICIENT OF A SINGLE CARBON NANOTUBE.....	25
B.	THERMAL CONDUCTIVITY OF TWO CARBON NANOTUBES	26
C.	EFFECTIVE THERMAL CONDUCTIVITY OF RANDOMLY ORIENTED CARBON NANOTUBES.....	28
V.	CONCLUSION/RECOMMENDATION.....	31
APPENDIX.	CNT MODELS.....	33
LIST OF REFERENCES.....		35
INITIAL DISTRIBUTION LIST		37

THIS PAGE INTENTIONALLY LEFT BLANK

LIST OF FIGURES

Figure 1.	Enhancement in thermal conductivity relative to pristine epoxy as a function of SWNT and VGCF loading (From Ref. [5])	3
Figure 2.	Thermal conductivity of CNT-epoxy composites magnetically processed at 0 and 25 T, compared with the neat epoxy control sample (also processed at 25 T) (From Ref. [6])	4
Figure 3.	Graphite layer with carbon atoms labeled using (n,m) notation[6]	17
Figure 4.	Geometric model two parallel (6, 6) armchair SWNT's	19
Figure 5.	1-D representation of 50 randomly dispersed SWNTs	20
Figure 6.	Geometric model (6, 6) armchair SWNT	21
Figure 7.	Non-bonded equilibrium distance between two (6, 6) CNTs oriented at various respective angles.	26
Figure 8.	Minimal potential energy separation distance as a function of orientation angle, θ	27
Figure 9.	Enhancement in effective thermal conductivity as a function of the number of CNTs	29
Figure 10.	Enhancement of effective thermal conductivity in the horizontal direction as a function of the total volume of CNTs with different CNT lengths	29
Figure 11.	Enhancement of effective thermal conductivity in the vertical direction as a function of the total volume of CNTs with different CNT lengths	30
Figure 12.	Enhancement of effective thermal conductivity in the horizontal and vertical direction as a function of the no. of CNTs linking the boundary.	30
Figure 13.	Relative Angle = 0°	33
Figure 14.	Relative Angle = 15°	33
Figure 15.	Relative Angle = 30°	33
Figure 16.	Relative Angle = 45°	33
Figure 17.	Relative Angle = 60°	33
Figure 18.	Relative Angle = 75°	33
Figure 19.	Relative Angle = 90°	34

THIS PAGE INTENTIONALLY LEFT BLANK

LIST OF TABLES

Table 1.	Optimized Parameters for the T-B Type Potential. [7].....	12
Table 2.	Thermal Conductivity of SWNTs.....	25
Table 3.	Lennard-Jones Potential Results for (6, 6) SWNT	26
Table 4.	Thermal Conductivity of Two (6, 6) SWNTs at Various Relative Angles.....	27
Table 5.	Material, Geometric Properties and Boundary Conditions for FEA.....	28

THIS PAGE INTENTIONALLY LEFT BLANK

ACKNOWLEDGMENTS

I would like to express my sincere gratitude to my advisor Prof. Young Kwon who never doubted my abilities to complete this thesis. I am greatly indebted to him for giving me the opportunity to work with him and for encouraging me throughout this process. His mentorship, guidance, and patience will never be forgotten.

I would like to thank my beautiful and intelligent wife, Lakeisha, for riding this rollercoaster with me. Thanks for your love, patience, and support.

Finally, I would like to acknowledge my source of inspiration and joy, my two year old son Emjay. Each day your smile and happiness encouraged me and reminded of what's truly important.

THIS PAGE INTENTIONALLY LEFT BLANK

I. INTRODUCTION

A. BACKGROUND

Since being discovered by Iijima in 1991 [1], carbon nanotubes (CNT's) have attracted worldwide attention in both research and industrial applications. Carbon nanotubes are long, thin cylinders of carbon macromolecules. They can be thought of as a sheet of graphite (hexagonal lattice of carbon) rolled into a cylinder with a typical diameter on the order of 0.14nm. The length of a single walled nanotube (SWNT) can be relatively large, up to several microns long. The strong sp^2 bonds of carbon nanotubes suggest an unusually high thermal conductance, expected to surpass that of monocrystalline diamond [2]. Unfortunately experimental attempts to quantify the heat transfer properties of SWNT have encountered many difficulties. However molecular dynamics (MD) simulations has proven to be a useful contributor to the ongoing catalog of CNT heat transfer properties.

The thermal conductivity is a thermophysical property of a material that indicates its ability to conduct heat. The magnitude of thermal conductivity varies over wide ranges for different materials. Thermal conductivity of a material depends on its chemical composition, physical structure, and state. In addition, it varies with the pressure and temperature at which the material is exposed. However, pressure is far less influential, so the dependence is tabulated as a function of temperature. In anisotropic materials, such as carbon nanotubes, the thermal conductivity also varies with direction. Given its small size and potentially high thermal conductivity, researchers have focused on this material as an efficient heat conductor in nanodevices and electronics.

Both diamond and in-plane graphite display very high thermal conductivities at moderate temperatures; for example 4900 and 3870 ($W m^{-1} K^{-1}$) at 173.2 K, respectively [3]. Both are made of a covalently bonded network of carbon atoms. Having a similar lattice structure, it is expected that carbon nanotubes will also have a high thermal conductivity. In fact many theoretical and experimental results suggest that the thermal conductivity of CNTs may be larger than those of both diamond and in-plane

graphite. Thus, an accurate evaluation of the thermal conductivity of nanotubes is an important step in the development of useful nanoscale devices.

Theoretical calculations have predicted the thermal conductivity of a single nanotube to be as high as $6600 \text{ W m}^{-1} \text{ K}^{-1}$ at room temperature [2]. However experimental measurements have not been as high. Experimental measurements of “mat” samples revealed a room temperature conductivity of approximately $35 \text{ W m}^{-1} \text{ K}^{-1}$ [4]. This degradation is due to the disordered and highly tangled nature of the sample. In addition, CNT has much lower thermal conductivity in the transverse direction than the longitudinal direction. These extreme differences in thermal conductivity are indicative of the fact that multiwalled nanotubes (MWNT), bundles and ropes exhibit varying degrees of thermal conductivity.

Recent publications have reported both thermal and electrical properties enhancements of single wall carbon nanotube-polymer composites. Scientific results show that these enhancements are a function of temperature, nanotube distribution and concentration. One report presented by Biercuk et al. [5] showed epoxy samples loaded with 1 wt% unpurified SWNT material increased thermal conductivity by 70% at 40K in comparison to pristine epoxy. The conductivity further increased to 125% at room temperature. Figure 1 illustrates the enhancement in thermal conductivity relative to pristine epoxy as a function of SWNT and vapor grown carbon fibers (VGCF).

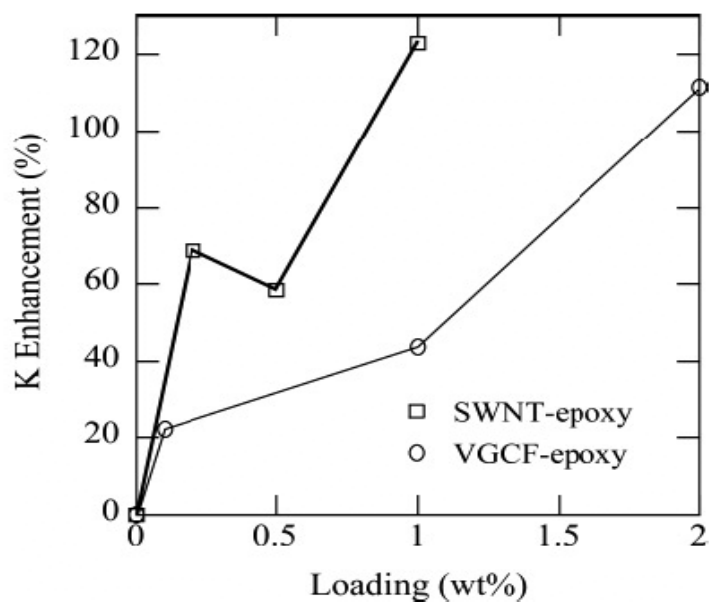


Figure 1. Enhancement in thermal conductivity relative to pristine epoxy as a function of SWNT and VGCF loading (From Ref. [5])

Meanwhile, researchers at Florida State University studied the effect of magnetic alignment on composite materials with 3 wt% SWNT loading. Even without magnetic field processing, the thermal conductivity increased by 300%. Magnetic alignment further increased the thermal conductivity by additional 10% [6].

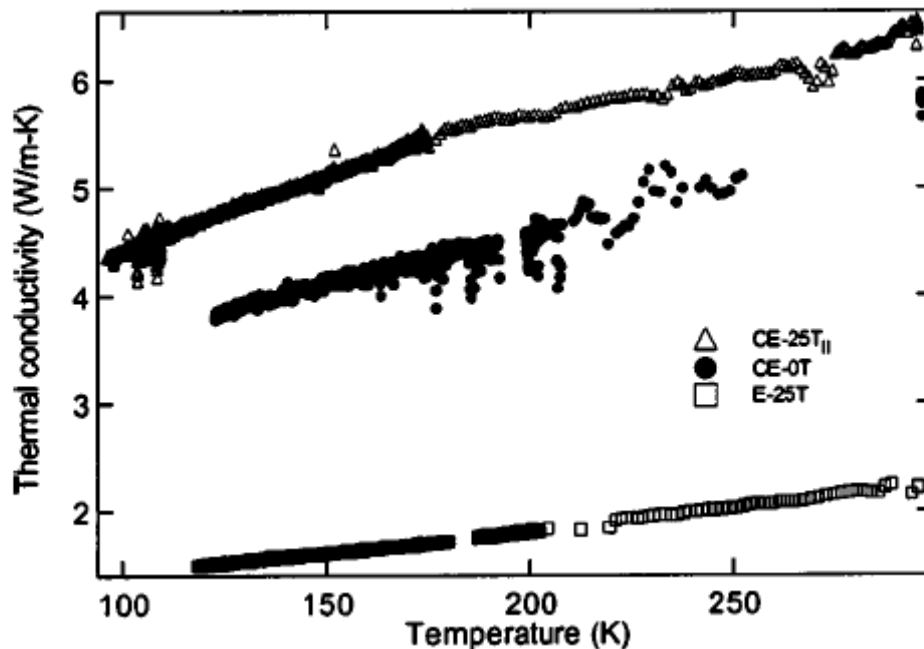


Figure 2. Thermal conductivity of CNT-epoxy composites magnetically processed at 0 and 25 T, compared with the neat epoxy control sample (also processed at 25 T) (From Ref. [6])

The above experimental observations provided significant evidence of the use of CNTs as a conductor of heat in composite materials, as well as in nano-scale devices. Thus, it is necessary to determine how orientation and dispersion affect heat conduction in nanotube systems. Fortunately, computational techniques for modeling and simulation which bridge continuum mechanics, quantum mechanics and molecular dynamics are available tools that predict and explain thermal properties of various CNTs.

B. OBJECTIVES

In this thesis, we employ a combination of the classical MD simulation method and the finite element method (FEM) to analyze the thermal conductivity in the longitudinal and transverse directions of randomly dispersed SWNTs.

To this aim, a multiscale analysis approach was adopted. At the nanoscale, molecular dynamics simulation was performed to determine the heat conduction coefficient of a single carbon nanotube using the Tersoff-Brenner potential [7]. Then, thermal conductivity of two carbon nanotubes positioned at different angles were studied after determining the equilibrium positions of the two nanotubes at various relative

positions using the Lennard-Jones pair potential for van der Waals interaction between adjacent SWNTs. Finally, using the data obtained in the previous analyses, the effective thermal conductivity of randomly oriented carbon nanotubes was calculated using the finite element method where each nanotube was modeled as a continuous rod. As a final step, an estimation of the validity of the molecular dynamics and FEM applied in this thesis is made by comparative analysis of the results with experimental data.

THIS PAGE INTENTIONALLY LEFT BLANK

II. MODELING, RELATED THEORY, AND METHODOLOGY

The properties exhibited by carbon nanotubes are highly dependent upon the basic geometrical structure of the molecule. Understanding of this dependence is an essential step in application of the MD simulation of a given CNT system. For example, the CNT structure should be analyzed in its lowest energy state. This chapter explains the synthesis of SWNTs, describes the basic structural properties of carbon nanotubes, and then presents the resultant initial geometrical models of SWNT which allow for the application of molecular dynamics and finite element modeling approach.

A. LABORATORY SYNTHESIS OF CARBON NANOTUBES

There are three common techniques used to produce carbon nanotubes of both the single-wall and multi-wall varieties: (1) arc discharge (2) laser ablation and (3) chemical vapor deposition. Purification of the tubes can be achieved by a variety of techniques: oxidation, acid treatment, annealing, sonication, and filtering and functionalisation techniques. There are pros and cons to be considered for each of these techniques. However the ultimate goal is to create an economically feasible large scale production technique that yields replicable pure results. Pure nanotubes are essential to the development and functionality of nano-devices and composite materials. It is widely accepted in the nanotechnology field that impure, flawed nanotubes have significantly degraded physical properties in comparison to pure nanotubes.

The arc discharge method is the most common and simplest way to produce carbon nanotubes. However the product consists of a mixture of components and requires separating nanotubes from the byproducts of the reaction. This method creates nanotubes through arc-vaporization of two carbon rods placed end to end, separated by approximately 1mm, in an enclosure that is usually filled with inert gas (helium, argon) at low pressure (between 50 and 700 mbar). A direct current of 50 to 100 A driven by approximately 20 V creates a high temperature discharge between the two electrodes. The discharge vaporizes one of the carbon rods and forms a small rod shaped deposit on the other rod. Producing nanotubes in high yield depends on the uniformity of the plasma arc and the temperature of the deposit form on the carbon electrode.

The laser ablation method is similar to the arc discharge method in that the reaction takes place in the presence of an inert gas and a catalyst. In this method, graphite electrodes are vaporized by a laser in an oven of 1200°C. The oven is filled with the inert gas to limit the pressure of the reaction. As the laser makes contact with graphite, a hot vapor plume forms, expands and cools rapidly. As the vaporized particles cool, small carbon molecules and atoms condense to form a mixture of carbon nanotubes and carbon nanoparticles. The use of pure graphite electrodes yields MWNTs; and SWNTs can be synthesized from a mixture of graphite and Co, Ni, or Fe. Laser vaporization results in a higher purer yield of SWNTs than those produced by the arc discharge method.

The third method, chemical vapor deposition (CVD) synthesis requires a gaseous form of carbon such as methane or carbon monoxide and an energy source, such as plasma. The energy source is used to separate the carbon molecule into reactive atomic carbon. The carbon then diffuses towards a pre-treated substrate, where the atoms combine to form the carbon nanotubes. Growth of SWNTs or MWNTs is controlled by applying an appropriate catalyst to the substrate.

The exact mechanism by which CNT's are formed is not known. However the three synthesis techniques all require a carbon based precursor, a catalysis, and intense, high energy reaction conditions.

B. MD THEORY AND TERSOFF-BRENNER (T-B) POTENTIAL

1. Validity of the Classical MD Simulation Method

In molecular dynamics (MD) simulations, atoms are treated as discrete particles whose trajectories are calculated by numerically integrating classical equations of motion subject to some given interatomic forces. The interatomic interactions are calculated from one of two methods. The first approach requires a summation of nuclear repulsions combined with electronic interactions determined from first principles. This method is commonly referred to as a quantum mechanical MD because it considers the influence electrons have on physical properties. Quantum MD simulations are computationally more difficult and time consuming because of the inclusion of electron interactions. In the second approach, quantum mechanical electrons are ignored. The energy and interatomic forces are a function of atomic position only. This approach is known as

classical MD, and is suitable for analyzing the mechanical properties of molecules when quantum effects are not significant. Under the appropriate assumptions energetically stable structures like carbon nanotubes can be modeled with the classical approach using Newton's second law, the Hamiltonian equation of motion, and an appropriate potential energy function. In this thesis, the classical MD simulation method was employed to calculate the thermal conductivity of a SWNT.

2. Newton-Hamiltonian Dynamics for the Classical MD Simulation

In the classical molecular dynamics method, the equations of motion (Newton's 2nd Law) are solved for atoms as:

$$F_i = m\ddot{r}_i = m \frac{d^2 r_i}{dt^2} \quad (1)$$

Here r_i and F_i are position vector, and force vector of atom i . The position vector locates the atom with respect to the origin of the coordinate system. The mass is assumed to be independent of position velocity, and time.

For an isolated system, the total energy E is conserved. Therefore, we can identify the total energy as the Hamiltonian H . For N-atoms, H takes the form:

$$H(r_i, p_i) = \frac{1}{2m} \sum_i^N p_i^2 + U(r_i) = E \quad (2)$$

where p_i is the momentum of an atom and the potential energy U results from interatomic interactions. Taking the derivative of equation (2) with respect to the position r , the explicit relationship between the Hamiltonian and the potential energy is:

$$\frac{\partial H}{\partial r_i} = \frac{\partial U}{\partial r_i} \quad (3)$$

Therefore, the resultant Hamilton's equations of motion are:

$$\frac{\partial H}{\partial p_i} = \frac{p_i}{m} = \dot{r}_i \quad (4)$$

$$\frac{\partial H}{\partial r_i} = -\dot{p}_i = -m\ddot{r}_i \quad (5)$$

Substituting equation (3) into equation (5) Newton's law becomes:

$$F_i = -\frac{\partial H}{\partial r_i} = -\frac{\partial U}{\partial r_i} \quad (6)$$

Equations (6) shows any conservative force can be written as the negative gradient of some potential energy function U , and the forces from all of the other atoms determine the accelerations of each atom in the given system [8].

3. Tersoff-Brenner (T-B) Type Potential

To model the bonded interaction among the carbon atoms of the nanotube, the classical Tersoff-Brenner potential was used [7]. The Tersoff-Brenner potential is specially suited for carbon-based systems and has been used in a wide variety of applications yielding results in agreement with experimental observations [9].

A universal analytic many-body force field function that works for all materials in all scenarios does not currently exist. However, the Tersoff-Brenner potential for carbon-based systems allows for reactive short-range bonded interactions. Specifically, chemical bonds can form and break during the course of the simulation. This significant advantage was contributed by Brenner when he introduced a bond function to Tersoff's original analytic potential energy function [10]. The resulting empirical equation is a pair wise exponential potential function of the atomic separation, angle, and the number of bonds given by:

$$U = \frac{1}{2} \sum_i u_i \quad (7)$$

$$u_i = \sum_{j \neq i} [V_R(r_{ij}) - B_{ij} V_A(r_{ij})] \quad (8)$$

where the repulsive and attractive pair terms. V_R and V_A are given by:

$$V_R(r_{ij}) = f_{ij}(r_{ij}) D_{ij}^{(e)} / (S_{ij} - 1) \cdot \exp\left(-\sqrt{2S_{ij}} \beta_{ij} (r - R_{ij}^{(e)})\right) \quad (9)$$

$$V_A(r_{ij}) = f_{ij}(r_{ij}) D_{ij}^{(e)} S_{ij} / (S_{ij} - 1) \cdot \exp\left(-\sqrt{2/S_{ij}} \beta_{ij} (r - R_{ij}^{(e)})\right) \quad (10)$$

D, S, β, R are empirical parameters given in Table 1, and the function $f_{ij}(r)$, restricts the pair potential to nearest neighboring atoms, given by:

$$f_{ij}(r) = \begin{cases} 1, & r < R_{ij}^{(1)} \\ \left[1 + \cos \left(\frac{\pi (r - R_{ij}^{(1)})}{R_{ij}^{(2)} - R_{ij}^{(1)}} \right) \right] / 2, & R_{ij}^{(1)} < r < R_{ij}^{(2)} \\ 0, & r < R_{ij}^{(2)} \end{cases} \quad (11)$$

B_{ij} represents a many-body coupling between the bond from atom i to atom j and the local environment of atom i .

$$B_{ij} = \left[1 + \sum_{k(\neq i, j)} G_i(\theta_{ijk}) f_{ik}(r_{ik}) \cdot \exp[\alpha_{ijk} \cdot ((r_{ij} - R_{ij}^{(e)}) - (r_{ik} - R_{ik}^{(e)}))] \right]^{-\delta_i} \quad (12)$$

$$G(\theta_{ijk}) = a_0 \left\{ 1 + \frac{c_0^2}{d_0^2} - \frac{c_0^2}{\{d_0^2 + (1 + \cos \theta)^2\}} \right\} \quad (13)$$

G is a function of θ , the angle between atoms $i - j$ and $i - k$ bonds and other constant variables. These equations require a total of 11 fitting parameters for carbon atoms. The values assigned to each of these parameters are given in Table 1, where the subscripts “cc” means that those parameters are used for just carbon-carbon bonding network without other elements such as hydrogen.

Table 1. Optimized Parameters for the T-B Type Potential. [7]

Parameter	Value	Parameter	Value	Parameter	Value
$R_{cc}^{(e)}$	1.42 Å	α_{ccc}	0.0	d_0^2	3.5^2
$D_{cc}^{(e)}$	6.0 eV	$R_{cc}^{(1)}$	1.7 Å		
β_{cc}	2.1 Å	$R_{cc}^{(2)}$	2.0 Å		
S_{cc}	1.22	a_0	0.00020813		
δ_{cc}	0.5	c_0^2	330^2		

The T-B potential energy function of two carbon atoms can be plotted as a continuous function from equations (9) through (15). The effective carbon bond length, $r_0 \sim 1.42 \text{Å}$ is the equilibrium separation distance between two carbon atoms. The equilibrium of two carbon atoms corresponds to the minimum potential energy of the system. In order for any CNT structure to form, the potential energy per each carbon atom must attain a minimum energy value. This minimum energy is defined as the bond energy and is known to be $\varepsilon \sim 2.5 \text{eV}$ for the carbon-carbon bond of CNTs. This value is consistent with experimental values of C-C tight bonding overlap energy [11].

The concept of bond formation occurring at the lowest potential energy is consistent throughout the world of chemistry. A bounded system, such as a carbon nanotube, has a lower potential energy than its constituent parts, which is what keeps the system together. The carbon atoms exert a force on each other in order to position themselves in the lowest potential energy state, graphically shown as the bottom of the potential well. This force is equivalent to the negative gradient of the potential energy function U given in equation (8).

4. Gear's Predictor-Corrector Method for Solving the EOM

All MD calculations require accurate and stable integrators in order to solve the equations of motion. Integrators are evaluated by stability and the ability to reproduce certain time and space correlations to a sufficient degree of accuracy. The Beeman algorithm and Verlet leap-frog method are classical finite difference approaches. The velocity of each molecule is calculated first, followed by the position of the molecule. However, in molecular dynamics, the motion of a particle is over a very large number of time steps, and the elaborate integration schemes of the Gear's Predictor-Corrector method has proven to be more accurate in each time step.

Gear's Predictor-Corrector algorithms consist of three steps; prediction, evaluation, and correction:

a. Prediction

From the positions and their time derivatives up to a certain order (fifth-order in this case), all known at time t , one "predicts" the same quantities at time $t + \Delta t$ by means of a Taylor expansion. Among these quantities are acceleration, velocity and position of the carbon atom.

$$r_i(t + \Delta t) = r_i(t) + \dot{r}_i(t)\Delta t + \ddot{r}_i(t)\frac{(\Delta t)^2}{2!} + \ddot{\dot{r}}_i(t)\frac{(\Delta t)^3}{3!} + r_i^{(4)}(t)\frac{(\Delta t)^4}{4!} + r_i^{(5)}(t)\frac{(\Delta t)^5}{5!} \quad (14)$$

$$\dot{r}_i(t + \Delta t) = \dot{r}_i(t) + \ddot{r}_i(t)\Delta t + \ddot{\dot{r}}_i(t)\frac{(\Delta t)^2}{2!} + r_i^{(4)}(t)\frac{(\Delta t)^3}{3!} + r_i^{(5)}(t)\frac{(\Delta t)^4}{4!} \quad (15)$$

$$\ddot{r}_i(t + \Delta t) = \ddot{r}_i(t) + \ddot{\dot{r}}_i(t)\Delta t + r_i^{(4)}(t)\frac{(\Delta t)^2}{2!} + r_i^{(5)}(t)\frac{(\Delta t)^3}{3!} \quad (16)$$

$$\ddot{\dot{r}}_i(t + \Delta t) = \ddot{\dot{r}}_i(t) + r_i^{(4)}(t)\Delta t + r_i^{(5)}(t)\frac{(\Delta t)^2}{2!} \quad (17)$$

$$r_i^{(4)}(t + \Delta t) = r_i^{(4)}(t) + r_i^{(5)}(t)\Delta t \quad (18)$$

$$r_i^{(5)}(t + \Delta t) = r_i^{(5)}(t) \quad (19)$$

b. Evaluation

The interatomic force F_i on each atom is computed taking the gradient of the potential at the predicted positions. The force on each atom is given by equation (20), where $U(r_{ij})$ is the continuous potential energy function that acts between atoms i and j . The resulting acceleration will be in general different from the "predicted acceleration". The difference between the two constitutes an "error signal".

$$F_i = -\sum_{j \neq i} \frac{\partial U(r_{ij})}{\partial r_{ij}} \quad (20)$$

c. Correction

This error signal $\Delta \ddot{r}_i$ is used to "correct" positions and their derivatives. All the corrections are proportional to the error signal, the coefficient of proportionality being a "magic number" determined to maximize the stability of the algorithm [12].

$$\Delta \ddot{r}_i = \left[\ddot{r}_i(t + \Delta t) - \ddot{r}_i^P(t + \Delta t) \right] \quad (21)$$

5. Simulation Time Step

By iterating the three steps of Gear's method at every time step, the MD simulation is propagated through time at intervals of Δt . Using the relationship between bond length r_o and the bond energy ε , a reasonable simulation time step Δt of 0.01 ps was estimated for the MD simulation. The methods required for this estimation are outlined below.

The kinetic energy of an atom in an isolated system should be approximately equal to the potential energy of the atom. Assuming that one atom can move within the bond length r_o during the time step, then the kinetic energy and the velocity v of the atom is written as:

$$E_k = \frac{1}{2}mv^2 = \varepsilon \quad (22)$$

$$v = \frac{r_o}{\Delta t} \quad (23)$$

From equations (22) and (23), the maximum possible time step value is given by:

$$\Delta t = r_o \sqrt{m / 2\varepsilon} \leq 0.02 \text{ ps} \quad (24)$$

where m is the mass of the carbon atom, and r_o and ε the carbon bond length and C-C tight bonding overlap energy. Equation (24) confirms that $\Delta t = 0.01ps$ is a reasonable time step for the MD code.

C. EQUILIBRIUM MOLECULAR DYNAMICS USING AUTO-CORRELATION FORMULA (GREEN-KUBO FORMULA)

This section describes the method of calculating thermal conductivity of a SWNT by introducing a heat flux autocorrelation function. Fourier's law, which describes macroscopic thermal conduction, is not appropriate for low-dimensional nano systems. Fourier's law states that the heat flux \mathbf{j} is related to the temperature gradient as $\mathbf{j} = -k \nabla T$, where k is the thermal conductivity tensor and T is the temperature distribution. Therefore a simple approach to studying thermal conduction in SWNTs is to apply a temperature gradient, measure heat flux along the axial direction, then calculate the thermal conductance. However the linearity between heat flux and temperature gradient as defined by Fourier's law does not hold due to the small dimensions of a CNT. Therefore the Green-Kubo fluctuation-dissipation theorem [13] is employed in this work.

In an equilibrium system, Green-Kubo formula takes the form:

$$\kappa = \frac{1}{k_B T^2 V} \int_0^\infty \langle J(t) J(0) \rangle dt \quad (25)$$

where k_B is the Boltzmann constant, V is the volume, T is the temperature of the sample and the angular brackets denote an ensemble average. The microscopic heat flux vector $J(t)$ is defined by:

$$J(t) = \frac{d}{dt} \sum_i r_i(t) \varepsilon_i(t) \quad (26)$$

where $r_i(t)$ is the time-dependent coordinate of atom i . According to the MD theory, the total potential energy can be expressed as a sum of binding energies of individual atoms, therefore the site energy $\varepsilon_i(t)$ can be taken to be:

$$\varepsilon_i = \frac{1}{2} m_i v_i^2 + \frac{1}{2} \sum_j u(r_{ij}) \quad (27)$$

In the above equation, v_i represents the velocity vector and $u(r_{ij})$ is the Tersoff-Brenner potential function described previously.

Generally two physical mechanisms contribute to thermal conduction in CNTs: (i) electron-phonon interactions, which depend on electronic band structures and the electron scattering process and (ii) phonon-phonon interactions, which depend on the vibrational modes of the lattice [14]. For CNTs, the electronic contribution to the thermal conductivity is negligible due to the low density of free charge carriers [15]. Phonon-phonon interactions dominate the overall thermal conductivity and can be studied by classical MD

D. LENNARD-JONES POTENTIAL

Non-bonded intermolecular interaction of carbon atoms in SWNT's can be represented by the Lennard-Jones potential. The Lennard-Jones potential is a simple mathematical model that represents two distinct forces of neutral atoms or molecules. When the separation r between the two molecules is small, Pauli repulsive forces dominate resulting in strongly positive potential. In contrast, when the separation r increases an attractive force known as van der Waals dominates. The general equation is expressed as:

$$V(r) = 4\varepsilon \left[\left(\frac{\sigma}{r} \right)^{12} - \left(\frac{\sigma}{r} \right)^6 \right]$$

where, r is the distance between interacting atoms, ε and σ are Lennard-Jones parameters for energy and equilibrium distance respectively. For carbon atoms the Lennard-Jones parameters are $\varepsilon = 0.00778$ kcal/mol and $\sigma = 3.4$ Å [16]. The Lennard-Jones model provides a smooth transition between (a) the attractive van der Waals force of an approaching pair of atoms from a certain distance and (b) the repulsive force when the distance of the interacting atoms becomes less than the sum of their contact radii. At equilibrium, the pair of atoms or molecules tends to go toward a separation corresponding to the minimum of the Lennard-Jones potential.

III. SIMULATION

A. MODELING OF SWNT AND BASIC STRUCTURES

1. Basic Structures of Carbon Nanotubes

Carbon nanotubes are long, thin cylindrical shell structures based on the hexagonal lattice structure of carbon allotrope, graphite. The length to diameter ratio can be extremely large, and the ends are “capped” with half-dome shaped fullerene molecules.

The single-walled carbon nanotube is considered to be the cornerstone of the nanotube family. Other known variants are multi-walled nanotubes (MWNT) and ordered SWNT arrays known as nanoropes. Most of the existing experimental methods have been successful at yielding MWNTs, however isolation of pure SWNTs have been the focus of many recent experimental techniques. If an adequate understanding of SWNTs is obtained, the cataloging of other variant properties will be much easier. The following outline will concentrate on the basic structural characteristics of SWNTs.

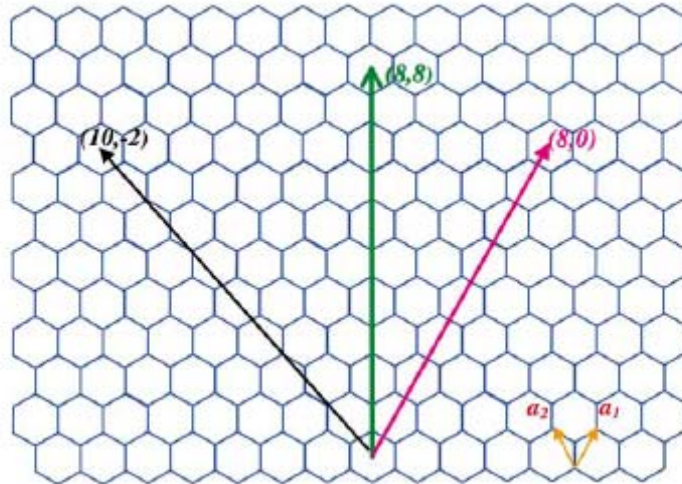


Figure 3. Graphite layer with carbon atoms labeled using (n,m) notation[6]

To understand the structural features of SWNT, Figure 3 shows a two dimensional honeycomb structure of a graphene sheet. The vectors shown represent the chiral vectors of a nanotube (\vec{C}). A chiral vector is defined as, $\vec{C} = n\vec{a}_1 + m\vec{a}_2$, where \vec{a}_1

and \bar{a}_2 are unit vectors. The vector represents two atoms in the graphene sheet, one of which serves as the origin. If the sheet is rolled until the two atoms coincide, the vector pointing from the first atom towards the other is the chiral vector and its length is equal to the circumference of the SWNT. Depending upon the combination of the indices (n, m) , three types of CNTs is possible. An (m, m) combination forms the “armchair” tube, $(n,0)$ is known as “zig-zag”, and (n, m) refers to a chiral nanotube. The pseudonym illustrates the shape of the nanotube perpendicular to the tube axis

The physical properties of carbon nanotubes are largely determined by the chiral indices (n, m) . The diameter of nanotubes, d_t expressed as a function of n and m is given by the following equation.

$$d_t = \frac{0.246}{\pi} \sqrt{(n^2 + n \cdot m + m^2)} \quad (nm) \quad (28)$$

The chiral angle is the angle between \bar{C} and \bar{a}_1 , given by equation (29).

$$\theta = \sin^{-1} \left\{ \frac{3^{1/2} \cdot m}{2(n^2 + n \cdot m + m^2)^{1/2}} \right\} \quad (29)$$

In addition, a SWNT can be either a metal, semiconductor or small-gap semiconductor depending on the (n, m) combination. For instance, nanotubes with $m - n \neq 3 \times \text{integer}$ results in a semi-conducting nanotube. Nanotubes with $m - n = 3 \times \text{integer}$, is found to be metallic[17]. Although these characterizes are very important to the study of electronic properties of SWNT, only a weak dependence of thermal conductivity can be contributed to chirality[18].

2. SWNT Model

Three models of SWNTs were created in order to analyze the heat transfer properties. A single $(6, 6)$ armchair CNT was modeled in order to determine the thermal conductivity of a typical SWNT. A second CNT, of equivalent dimensions was then created to analysis the effects of intermolecular forces on thermal conductivity. Figure 4 shows the side view of two parallel SWNTs each consisting of 366 carbon atoms, which are represented by individual circles through the visualization MATLAB algorithm.

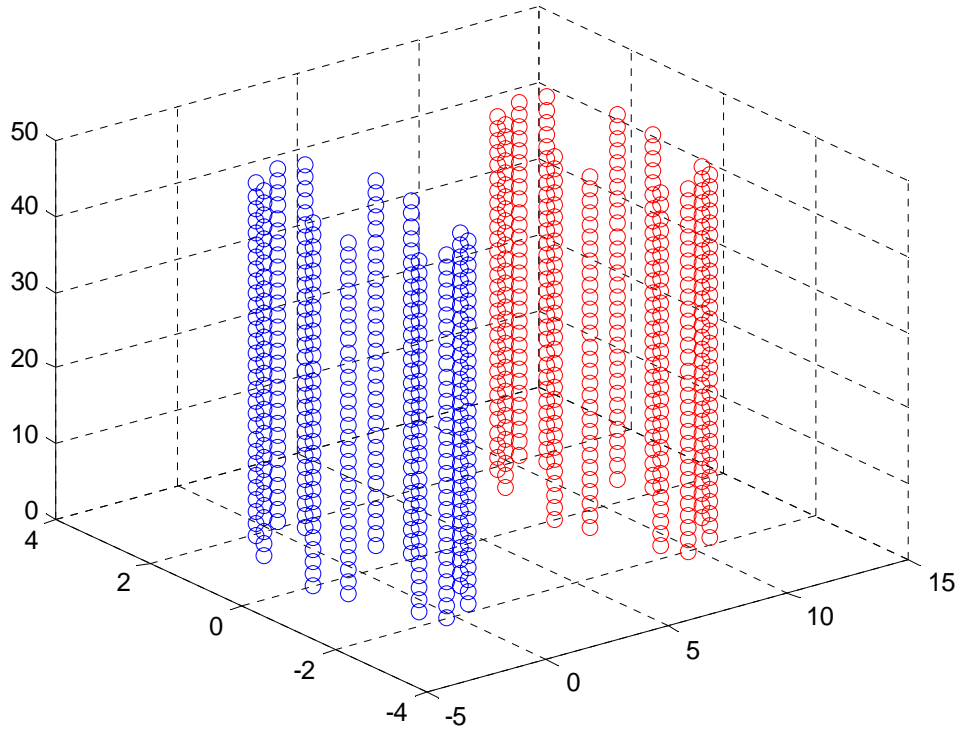


Figure 4. Geometric model two parallel (6, 6) armchair SWNT's

The C-C distance used in this model is 1.421 \AA , and the radius of the tube is 4.07 \AA . The length to diameter ratio was limited to 5:1 in order to decrease computational costs. A third model was created to determine the effective thermal conductivity of randomly dispersed SWNTs. The CNT's are represented as 1-D rods randomly oriented in unit square. Figure 5 shows a typical dispersion of 50 SWNT with nondimensional length of 0.5.

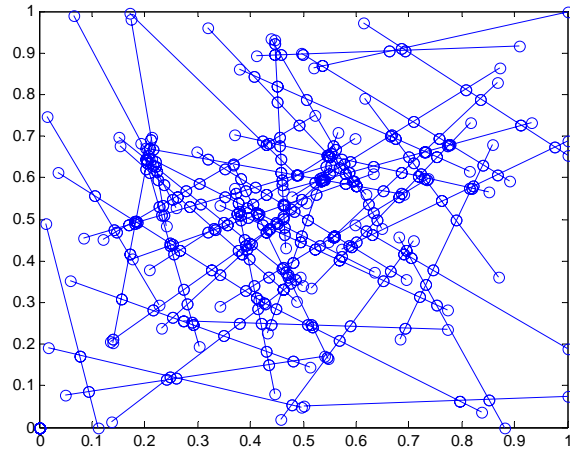


Figure 5. 1-D representation of 50 randomly dispersed SWNTs

B. SIMULATION PROCEDURES

All programming language required for the computer simulations in this study were written using Mathworks-MATLAB. MATLAB is a high-level technical computing language and interactive environment for algorithm development, data visualization, data analysis, and numeric computation.

1. Thermal Conductivity Coefficient of a Single Carbon Nanotube

An armchair (6, 6) SWNT structure was modeled, having a diameter of 8.14 Å and length to diameter ratio of 5:1. The model consisted of 366 atoms.

Armchair (6,6) SWNT, No. Atoms = 294

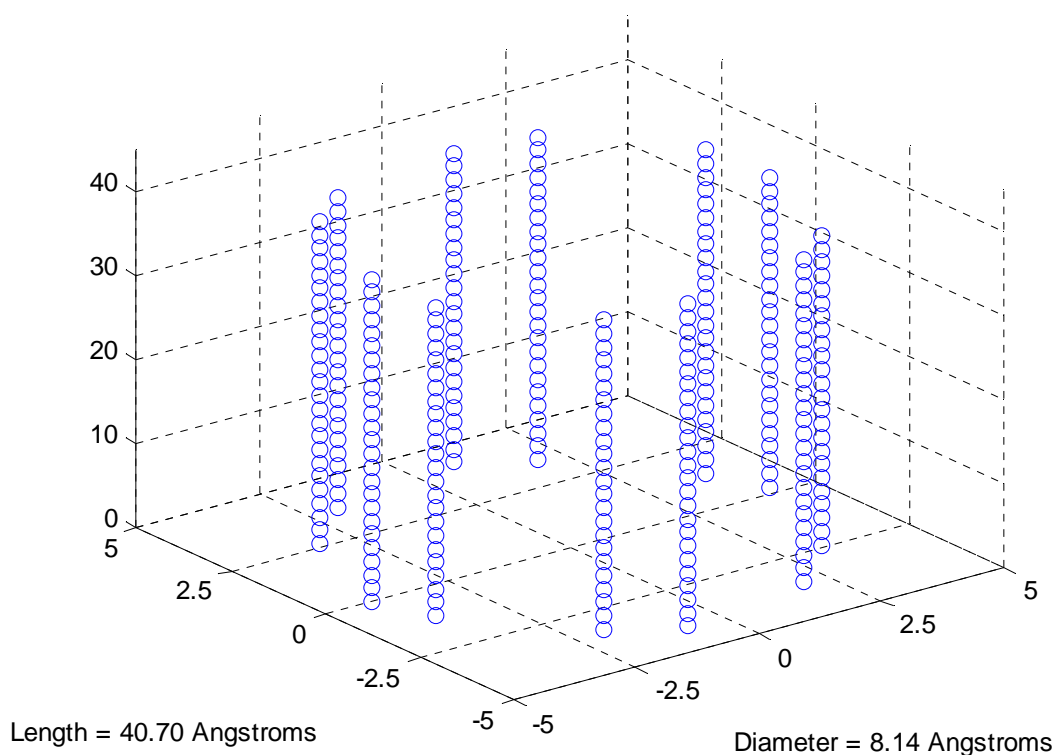


Figure 6. Geometric model (6, 6) armchair SWNT

In this molecular dynamics simulation program, the Tersoff Brenner potential was employed as the potential function with the parameters set to those outlined in Table 1. The Gear's Predictor-Corrector method was adapted to integrate the equation of motion with each run consisting of 10000 time steps of 0.01 ps. Periodic boundary conditions were used to model the microscopic system. The thermal conductivity coefficient in both the axial and radial direction was found from the Green-Kubo autocorrelation function outlined in equation (25).

2. Thermal Conductivity of Two Carbon Nanotubes

Prior to determining the thermal conductivity of two adjacent SWNTs, the non-bonded equilibrium distance was determined from the Lennard-Jones potential function. For this simulation two equivalent armchair (6, 6) SWNTs were modeled. The equilibrium position was determined by incrementally increasing the relative distance between the two CNTs from 0 to 10 while simultaneously calculating the LJ potential for

the system. These measurements were calculated at fixed relative angles of 15, 25, 30, 45, 60, 75 and 90 degrees. The equilibrium position was then used in the determination of the thermal conductivity of two adjacent SWNTs. The molecular dynamic methods described in section one were simply repeated for two adjacent CNTs. By doing so, the affect of non-bonded carbon-carbon interactions is represented in the longitudinal and transverse thermal conductivities calculations.

3. Effective Thermal Conductivity

The effective thermal conductivity of randomly oriented carbon nanotubes was calculated using finite element analysis. Unlike macroscopic three-dimensional material, carbon nanotubes can be thought of as quasi one-dimensional rods. Therefore, to simulate thermal contact between adjacent SWNTs each nanotube was modeled as a continuous rod. The total number of tubes was varied between 25 and 100 in increments of 25. Additionally, the non-dimensional length of the CNT was set at 0.5, 0.6, 0.7, and 0.8 to determine the effect length has on thermal conductivity. Finally, the non-dimensional lengths were decreased by 50% while doubling the number of CNTs. This procedure allowed for the analysis of tube length while keeping the total volume of CNTs constant. The thermal conductivity values determined in the first MD simulation is used to describe the material properties of randomly dispersed nanotubes in this final simulation.

MATLAB's "rand" function was used to generate random position coordinates of the initial tube. Subsequent tubes were then added in a random manner. Concurrently, the tubes were normalized and repositioned to ensure that they remained within the domain of a unit square. To ensure percolation between the temperature boundary conditions and to prevent the generation of an isolated tube, each tube was required to overlap with another tube within the confines of the unit square. Conventional finite element procedures were then employed for the heat conduction analysis.

For finite element analysis of microscale heat transfer of CNTs, nodal coordinates were extracted from the end point coordinates of the 1-D rods as well as from the intersecting coordinates of the randomly overlapped tubes. Hence, a truss element with two nodes was used to represent the basic CNT structure. From Fourier's law, the governing equation for one-dimensional heat flux can be written:

$$J = -kA\Delta T \quad (30)$$

where k is the thermal conductivity tensor, A is the cross section area, and T is the temperature distribution. The finite element formulation leads to a generic matrix equation in the form of

$$[K]\{u\} = \{F\} \quad (31)$$

K being the stiffness matrix, and u the temperature vector. The heat flux vector, F , represents the contributions of the heat source and the boundary conditions. Solving for the nodal temperatures, we are able to calculate horizontal and vertical heat flux of the unit square. The effective thermal conductivity was found by substituting the heat flux solutions into equation (30) and solving for the thermal conductivity coefficient.

THIS PAGE INTENTIONALLY LEFT BLANK

IV. RESULTS AND DISCUSSION

A. THERMAL TRANSFER COEFFICIENT OF A SINGLE CARBON NANOTUBE

In this work, several armchair CNTs are simulated.

Table 2. Thermal Conductivity of SWNTs

Armchair Indices	Longitudinal Direction	Reference Values	
(5,5)	3325.8 W/mK	~2300 W/mK [19]	~790 W/mK [20]
(6, 6)	3215 W/mK		
(8, 8)	1813 W/mK	250-350W/mK [21]	
(10, 10)	804.8 W/mK	215-831W/mK [22]	~2980 W/mK [23]

The simulation shows that the thermal conductivity is very high along the tube axis, $3325.8 \text{ W m}^{-1}\text{K}^{-1}$ for (5,5) CNT which is indicative the anisotropic nature of nanotubes. This value is comparable to those obtained by Osman et. al, whose MD simulation for (5, 5) SWNT yielded a value of $2300 \text{ W m}^{-1}\text{K}^{-1}$ [19]. The trend obtained from this simulation shows steady decline in thermal conductivity as the diameter of the nanotube increases. A similar observance is made by Osman and Srivastava for (5,5) and (10, 10) nanotubes. They found (5,5) nanotubes to provide the highest thermal conductivity at room temperature, as compared to (10, 10) and (15,15) nanotubes. It was suggested that the probability of Umklapp processes are higher in SWNTs of smaller diameters as compared to tubes of larger diameters [19]. The Umklapp processes describe the resistive phonon-phonon scattering process believed to limit thermal conductivity in crystalline materials.

Unfortunately there is little agreement on the specific thermal conductivity of a SWNT as indicated by table 2. Typical values obtained from MD simulations have ranged between 2000 and 6000 W/mK. Further investigation is required to explain the trends found in this simulation.

B. THERMAL CONDUCTIVITY OF TWO CARBON NANOTUBES

The non-bonded equilibrium distance between equivalent adjacent SWNTs was determined from the Lennard-Jones potential function. Figure 7 shows the LJ potential curve for a pair of armchair (6, 6) carbon nanotubes. The equilibrium distance values obtained are shown in Table 3.

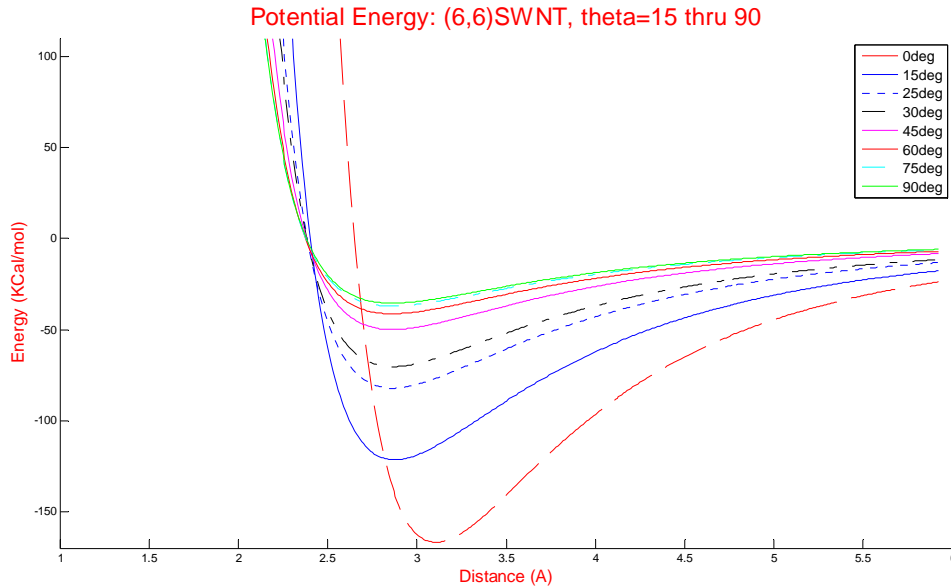


Figure 7. Non-bonded equilibrium distance between two (6, 6) CNTs oriented at various respective angles.

Table 3. Lennard-Jones Potential Results for (6, 6) SWNT

Relative Angle	Equilibrium Distance (Å)	Minimum Energy (Kcal/mol)
0°	3.1	7.228 eV
15°	2.86	5.271 eV
30°	2.86	3.052 eV
45°	2.84	2.167 eV
60°	2.86	1.792 eV
75°	2.86	1.606 eV
90°	2.86	1.538 eV

By plotting the minimum energy distance as a function of relative angle (Figure 8), it is apparent that beyond 15°, the relative angle does not have a significant effect on minimum energy position. This is to be expected because a cutoff distance of $r = 2.5\sigma$ was implemented to decrease the computation time of the LJ potential. As the angle is increased the number of atoms interacting becomes approximately equal. Although the above arguments are considered for only two nanotubes, similar arguments apply to the entire network of non-bonded nanotubes.

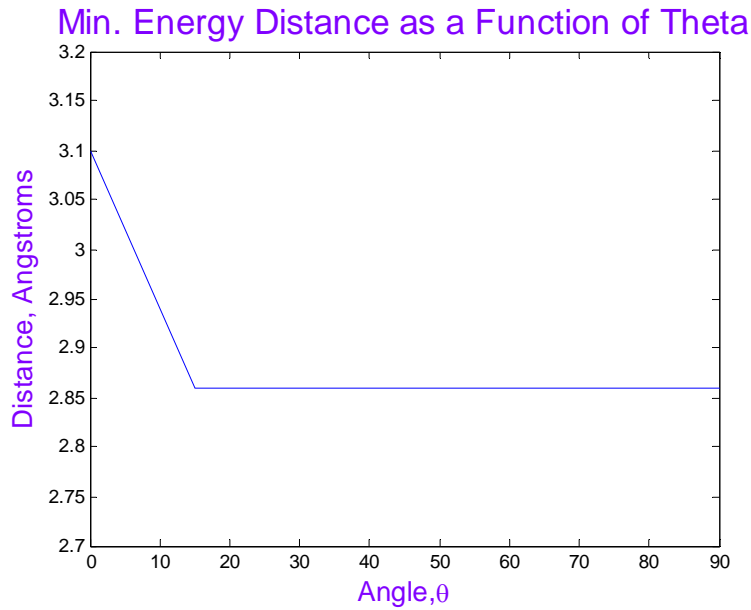


Figure 8. Minimal potential energy separation distance as a function of orientation angle, θ

Once the minimum equilibrium distance was obtained, the thermal conductivity of paired SWNTs is obtained by molecular dynamics simulation.

Table 4. Thermal Conductivity of Two (6, 6) SWNTs at Various Relative Angles

Angle	Thermal Conductivity
0°	15 W/mK
15°	20 W/mK
75°	15 W/mK
90°	10 W/mK

C. EFFECTIVE THERMAL CONDUCTIVITY OF RANDOMLY ORIENTED CARBON NANOTUBES

The longitudinal and transverse thermal conductivity values obtained from the molecular dynamic simulations conducted previously were used as material properties in the finite element analysis of the effective thermal conductivity of randomly dispersed SWNTs in a unit area.

Table 5. Material, Geometric Properties and Boundary Conditions for FEA

Conductivity in Axial Direction	3000 W/mK
Conductivity in Radial Direction	20 W/mK
Radius	0.01
Spacing	0.01
Tolerance	0.01-0.1
Boundary Temp. 1	100K
Boundary Temp 2	200K

In Figure 9, the effective thermal conductivity of the randomly dispersed nanotubes increases nonlinearly with nanotube loading. Figures 10 and 11 shows a steady increase in the effective thermal conductivity in both the horizontal and vertical directions of the unit square as the length and total volume of CNTs increase. In addition Figure 9 shows an increase in effective thermal conductivity with increasing tube length. Finally, Figure 12 shows a steady increase in effective thermal conductivity as the minimal number of CNTs linking the boundary is increased. Collectively these results show that the heat flux between boundaries increases with tube length and volume fraction. As the volume fraction of nanotubes increases, the number of interactions increases. In turn the effective conductivity increases due to more efficient percolation. The aforementioned behavior implies that thermal conductivity enhancement in nanotube suspensions will largely depend on length and concentration of nanotubes. The findings presented in this simulation are in agreement with experimental results published by Biercuk et al which show nonlinear increase in thermal conductivity with an increasing weight percentage of SWNT loaded epoxy [5].

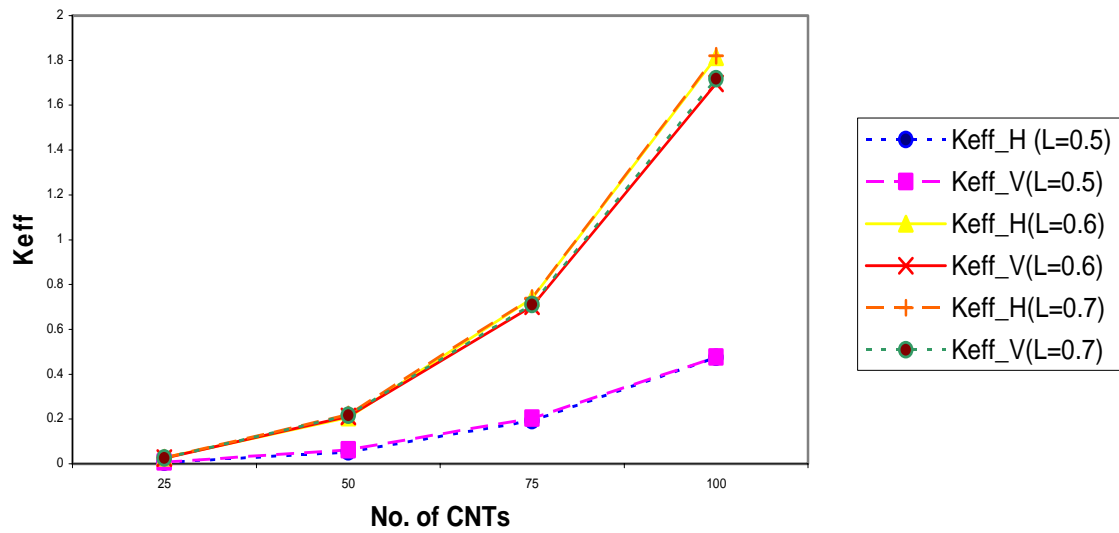


Figure 9. Enhancement in effective thermal conductivity as a function of the number of CNTs

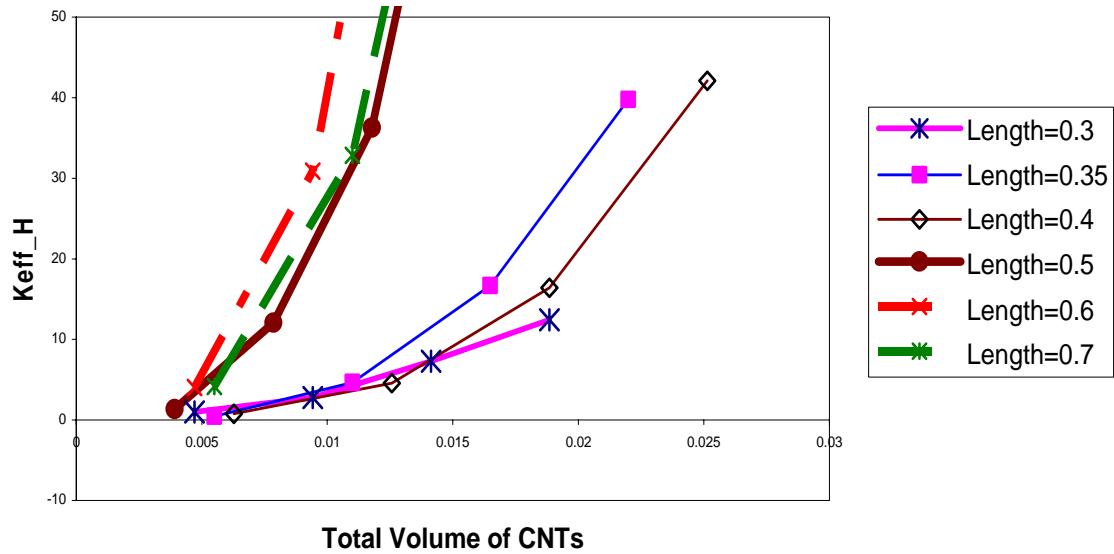


Figure 10. Enhancement of effective thermal conductivity in the horizontal direction as a function of the total volume of CNTs with different CNT lengths

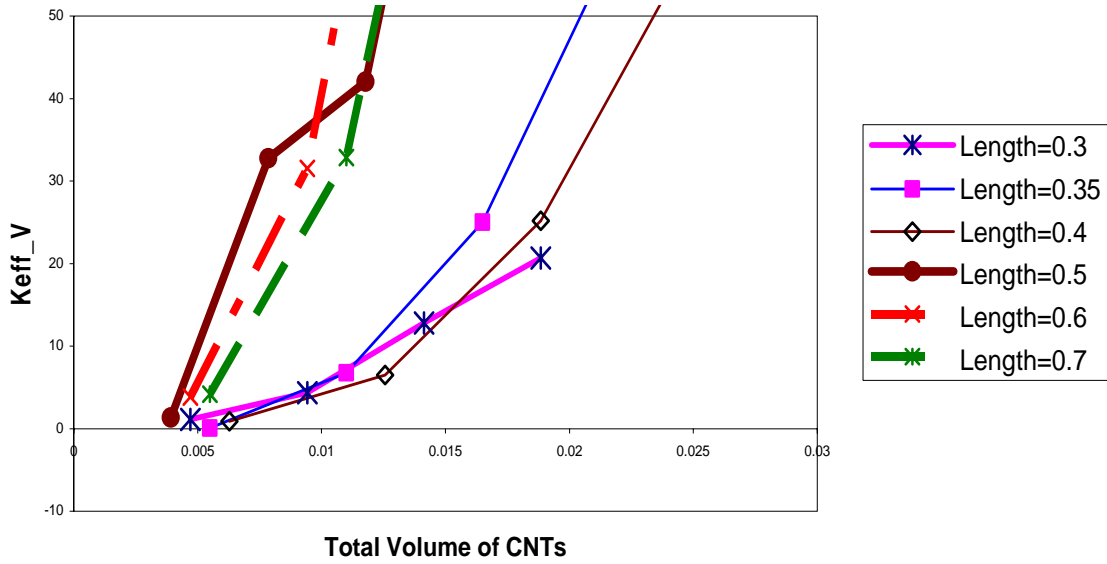


Figure 11. Enhancement of effective thermal conductivity in the vertical direction as a function of the total volume of CNTs with different CNT lengths

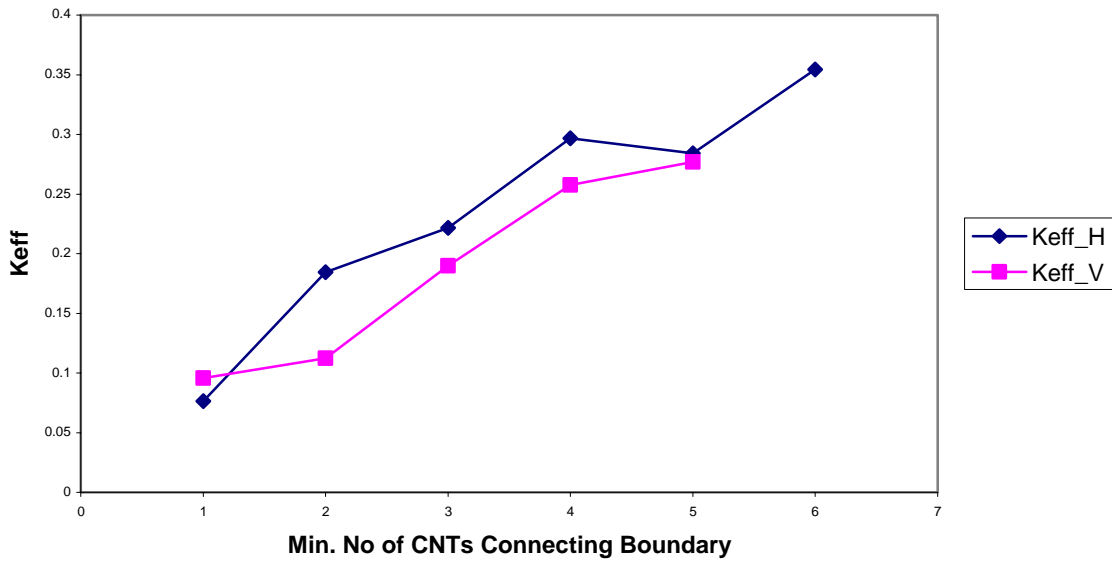


Figure 12. Enhancement of effective thermal conductivity in the horizontal and vertical direction as a function of the no. of CNTs linking the boundary.

V. CONCLUSION/RECOMMENDATION

The heat conduction coefficient of a single-walled carbon nanotube (SWNT) was simulated by the molecular dynamics method with the Tersoff-Brenner bond order potential. The results obtained from the simulation were then used as material properties in the finite element model of the effective thermal conductivity of randomly oriented carbon nanotubes. This method is based on a system of one-dimensional percolating rods that connect two reservoirs at different temperatures. The significant findings of this work were:

- A multiscale technique is useful to predict the effective thermal conductivity of randomly dispersed CNTs.
- The equilibrium distance between two adjacent CNTs remains almost the same as the relative angle varies.
- For the same size of CNTs, the effective thermal conductivity increases nonlinearly with the increasing number of CNTs.
- The effective thermal conductivity is significantly greater for longer CNTs as compared to shorter CNTs with the same total volume fraction.

The general trends resulting from these simulations indicate significant thermal conductivity enhancement when the tube length, volume fraction and number of CNTs linking the boundary is increased. These results support the very important implication of thermal enhancement in nanotube-based composite materials as well as nano-devices.

A few recommendations can be made for future studies based on the methods used and results obtained in this research.

- In reality, carbon nanotubes have defects and irregularities that decrease the thermal conductivity. Therefore vacancy concentrations should be incorporated in the simulation to determine its affect on thermal conductivity.
- Research has shown that magnetically aligned nanotubes in composite materials further enhance the thermal conductivity. The finite element model used here can be adjusted to investigate these findings further.

THIS PAGE INTENTIONALLY LEFT BLANK

APPENDIX. CNT MODELS

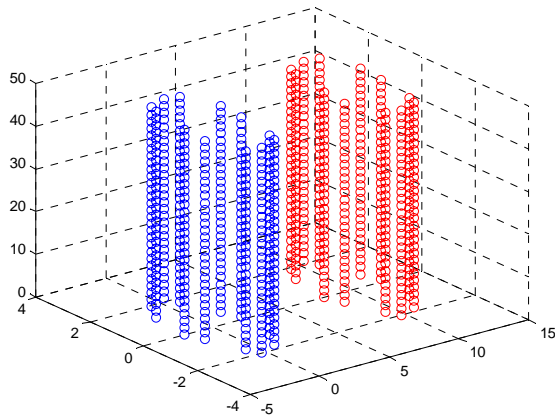


Figure 13. Relative Angle = 0°

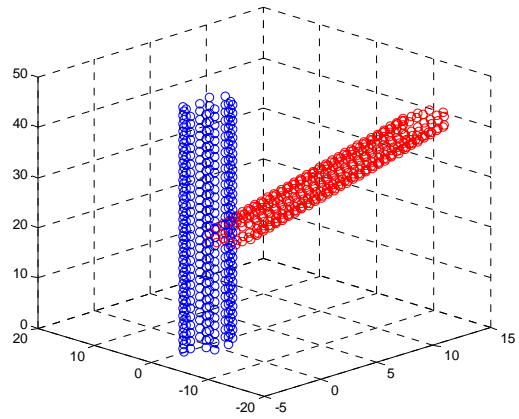


Figure 16. Relative Angle = 45°

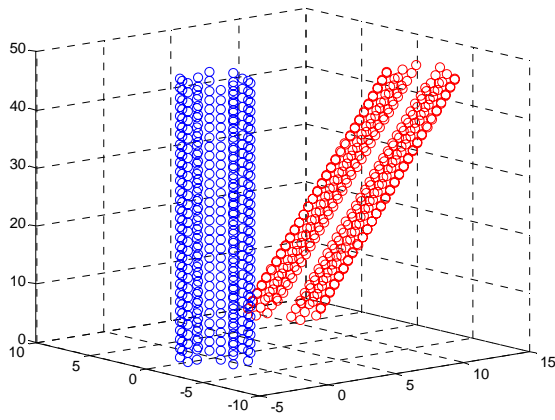


Figure 14. Relative Angle = 15°

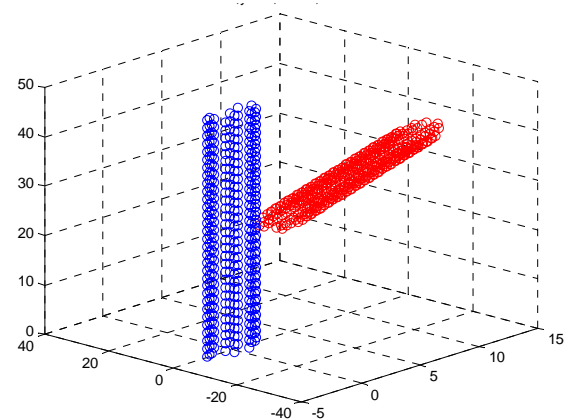


Figure 17. Relative Angle = 60°

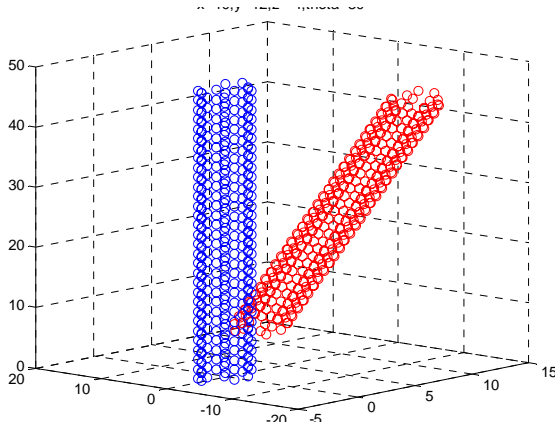


Figure 15. Relative Angle = 30°

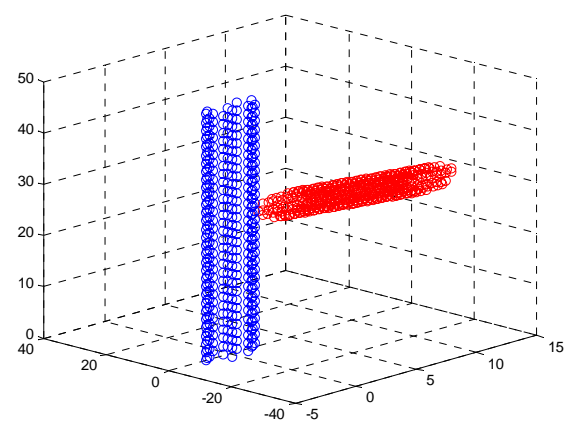


Figure 18. Relative Angle = 75°

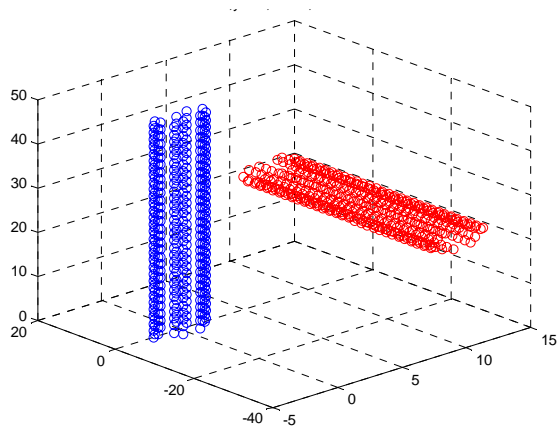


Figure 19. Relative Angle = 90

LIST OF REFERENCES

- [1] S. Iijima, 1991: Helical microtubes of graphite carbon. *Nature*. **354**, 56-58.
- [2] S. Berber, Y. Kwon, D. Tománek, 2000: Unusually high thermal conductivity of carbon nanotubes. *Phys. Rev. Lett.* **84**, 4613-4616.
- [3] G. W. C. Kaye and T. H. Laby, 1995: *Tables of Physical and Chemical Constants*, 16th ed. Longman, London.
- [4] J. Hone, M. Whitney, C. Piskoti, A. Zettl, 1999: Thermal conductivity of single-walled carbon nanotubes. *Phys. Rev. B* **59**, R2514-R2516
- [5]...M. J. Biercuk, M. C. Llaguno, M. Radosavljevic, J. K. Hyun, A. T. Johnson, and J.E. Fischer, 2002 Carbon nanotube composites for thermal management. *Appl. Phys. Lett.* **80**, 2767-2769.
- [6] E. S. Choi, J. S. Brooks, D. L. Eaton, M. S. Al-Haik, M.Y. Hussaini, H. Garmestani, D. Li, and K. Dahmen, 2203. Enhancement of thermal and electrical properties of carbon nanotube polymer composites by magnetic field processing. *J. of Appl. Phys.* **94**, 6034-6039.
- [7] D. W. Brenner, 1990: Empirical potential for hydrocarbons for use in simulating the chemical vapor deposition of diamond films. *Phys. Rev. B.* **42**, 9458-9471.
- [8] N. Hand, and J. D. Finch, 1998: *Analytical Mechanics*, Cambridge University Press, New York, 175 – 184
- [9] D. Srivastava, C. Wei, and K. Cho, 2003. Nanomechanics of carbon nanotubes and composites. *Appl. Mech. Rev.* **56**. 215-230.
- [10] R. Ruoff, D. Qian, and W. K. Liu, 2003. Mechanical properties of carbon nanotubes: theoretical predictions and experimental measurements. *C. R. Physique.* **4**, 993-1008.
- [11] W. G. Wilder, L. C. Venema, A. G. Rinzler, R. E. Smalley, and C. Dekker, 1998. Electronic structure of automatically reserved carbon nanotubes. *Nature* **291**, 6662.
- [12] J. M. Haile, 1997: *Molecular Dynamics Simulation: Elementary Methods*, John Wiley & Sons, Inc., New York, pp. 157-177.
- [13] R. Kubo, M. Toda and N. Hashitsume, 1985. *Statistical Physics II, Nonequilibrium Statistical Mechanics* Springer, New York.

- [14] Z. Yao, J. Wang, B. Li, and G. Liu, 2005. Thermal conduction of carbon nanotubes using molecular dynamics. *Phys. Rev. B.* **71**, 085417-1 – 085417-7.
- [15] P. J. Lin-Chung and A. K. Rajagopal, 1999: Theory of thermopower in disordered mixed crystals: Application to Si-Ge systems. *Phys. Rev. B* **60**, 12033.
- [16] C. Li and T. Chou, 2004: Vibrational behaviors of multiwalled-carbon-nanotube-based nanomechanical resonators. *Appl. Phys. Lett.* **84**, 121-123.
- [17] H. Dai, 2002. Carbon nanotubes: opportunities and challenges. *Surface Science.* **500**, 218-241.
- [18] M. Osman and D. Srivastava, 2001. Temperature dependence of the thermal conductivity of single-wall carbon nanotubes. *Nanotechnology.* **12**, 21-24.
- [19] M. Osman, and D. Srivastava, 2001: Temperature dependence of the thermal conductivity of single-wall carbon nanotubes, *Nanotechnology* **12**, 21–24.
- [20]...G. Zang, and B. Li, 2005. Thermal conductivity of nanotubes revisited: Effects of chirality, isotope impurity, tube length, and temperature, *Journal of Chemical Physics* **123**, 114714.
- [21] S. Maruyama, 2003. A molecular dynamics simulation of heat conduction of a finite length single-walled carbon nanotubes, *Micro. Therm. Eng.* **7**, 41-50.
- [22]...J. F. Moreland, J. B. Freund and G. Chen, 2004. The disparate thermal conductivity of carbon nanotubes and diamond nanowires studied by atomistic simulation, *Microscale Thermophysical Engineering* **8**, 61-69.
- [23] J. Che, T. Cagin, and W. A. Goddard III, 2000: Thermal conductivity of carbon nanotubes, *Nanotechnology* **11**, 65-69.

INITIAL DISTRIBUTION LIST

1. Defense Technical Information Center
Ft. Belvoir, Virginia
2. Dudley Knox Library
Naval Postgraduate School
Monterey, California
3. Young W. Kwon, Code ME/Kw
Department of Mechanical & Astronautical Engineering
Monterey, California
4. Eric D. Felder
Perry, Georgia